

Impact of Orientation Misalignments on Black Phosphorus Ultrascaled Field-effect Transistors

Cedric Klinkert, Sara Fiore, Jonathan Backmann, Youseung Lee, and Mathieu Luisier
Integrated System Laboratory, ETH Zurich, Switzerland (e-mail: cedrick@iis.ee.ethz.ch)

Abstract—Two-dimensional materials with strong bandstructure anisotropy such as black phosphorus (BP) have been identified as attractive candidates for logic application due to their potential high carrier velocity and large density-of-states. However, perfectly aligning the source-to-drain axis with the desired crystal orientation remains an experimental challenge. In this paper, we use an advanced quantum transport approach from first-principle to shed light on the influence of orientation misalignments on the performance of BP-based field-effect transistors. Both *n*- and *p*-type configurations are investigated for six alignment angles, in the ballistic limit of transport and in the presence of electron-phonon and charged impurity scattering. It is found that up to deviations of 50° from the optimal angle, the ON-state current only decreases by 30%. This behavior is explained by considering a single bandstructure parameter, the effective mass along transport direction.

Index Terms—2D materials, black phosphorus, transistors, bandstructure anisotropy, device simulation

I. INTRODUCTION

2D MATERIALS have received a wide attention from the scientific community ever since the discovery of graphene in 2004 [1]. The necessity of a band gap for logic applications ultimately led experimental efforts towards other 2D materials such as transition metal dichalcogenides (TMDs) e.g. MoS₂ [2] black phosphorus (BP) [3]–[5]. The latter material emerged as a serious contender due to its anisotropic bandstructure that simultaneously provides high carrier velocities and large density-of-states (DOS) [6]–[8], two properties that have been leveraged to design various types of more-than-Moore logic switches [9], [10].

Recent theoretical studies [11], [12] suggest that many other 2D materials with strong anisotropic conduction (CB) and/or valence band (VB) exist, e.g. Ag₂N₆, S₆Te₄Zr₂ or P₈Si₄. In their mono-layer form, when used as the channel material of ultra-scaled field-effect transistors, such compounds might exhibit almost ideal electrostatic characteristics as well as very high ON-state currents, if the transport direction is aligned with the proper crystal axes, i.e. the one with the lowest effective mass. However, from an experimental point of view, obtaining such perfect alignments is extremely challenging. If transport occurs along the crystal axis with the largest effective mass, device simulation predicts severe performance degradations for BP [13]–[15]. Most studies focused on the best- and worst-case scenarios, very few on what happens in between [16].

Here, we therefore study the impact of orientation misalignments on the ON-state current of ultra-scaled BP-FETs in their *n*- and *p*-type configuration. An advanced quantum

transport solver combining density-functional theory (DFT) and the Non-equilibrium Green's Function formalism (NEGF) is employed for that purpose. After introducing this simulation approach in Section II, it is revealed in Sections III that orientation misalignments up to 50° from the ideal case do not significantly alter the ON-state current of BP-FETs, with minor performance loss up to a misalignment angle of 20° . This behavior, which occurs both in the ballistic limit of transport and in the presence of electron/hole-phonon and charged impurity scattering, is explained based on the calculation of angle-dependent effective masses.

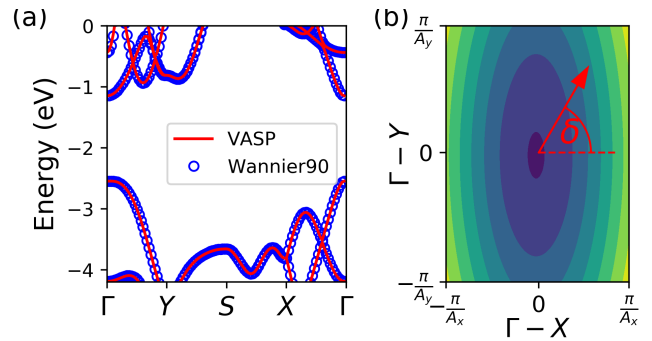


Fig. 1. (a) Electronic bandstructure of a BP monolayer as calculated with the VASP DFT code (red lines) and after transformation into a basis of maximally localized Wannier functions (blue circles). (b) Energy contour-plot of the lowest conduction band of BP. The red arrow indicates a transport direction with a misalignment angle δ with respect to the direction having the smallest transport effective mass.

II. APPROACH

The simulation results reported in this paper were obtained with an atomistic quantum transport solver [17] based on the NEGF equations following the same methodology as in [12]. An *ab initio* scheme is employed to capture the electronic band structure of BP and to create a suitable Hamiltonian matrix for the device geometry of interest. This step is achieved by converting the electronic structure received from a DFT package such as VASP [18] from a delocalized plane-wave basis to a set of maximally localized Wannier functions (MLWF) using the Wannier90 code [19]. The Hamiltonian of any unit cell can now be constructed by identifying the Wannier interaction for each atomic bond [20]. To minimize the computational burden, transport is evaluated along directions leading to reasonably small orthorhombic unit cells.

As exchange correlation functional the general gradient approximation of Perdew Burke Ernzerhof [21] is used. The PBE

band gap of BP, $E_{g,PBE} = 0.91 \text{ eV}$, is raised to the value obtained by the GLLBsc functional [22], $E_{g,GLLBsc} = 1.40 \text{ eV}$ to avoid artificial source-to-drain tunneling in the OFF-state. This increase is justified by the systematic underestimation of the semiconductor band gaps by the PBE functional. The resulting bandstructure of BP, before and after the MLWF transformation is shown in Fig. 1(a) demonstrating the accuracy of the approach. A contour plot of the lowest conduction band is depicted in Fig. 1(b). The optimal performance is obtained when the transport axis is aligned with the $\Gamma - X$ axis, while δ indicates the misalignment angle.

As scattering is known to influence electron and hole transport in BP transistors [6], [23], the NEGF model of [24] is adopted to account for these effects through dedicated self-energies. It combines charged impurity scattering (CIS), as defined in [25], and electron/hole-phonon interactions with *ab initio* inputs only, as described in [26]. Both the derivatives of the Hamiltonian matrix, which couple the electron/hole and phonon populations, and the phonon modes/frequencies are computed at the DFT level with VASP.

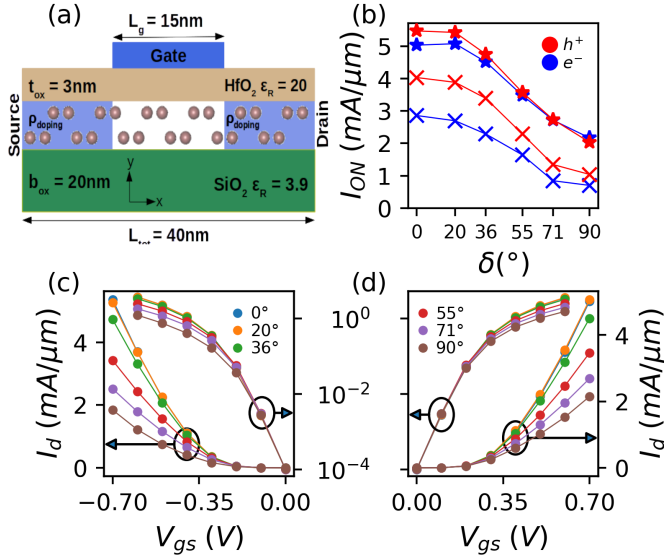


Fig. 2. (a) Schematic view of the simulated single-gate FET with a BP mono-layer as channel. (b) ON-state currents of all simulated transistors as a function of the misalignment angle δ , with (lines with crosses) and without (lines with stars) CIS and electron/hole-phonon scattering. (c) Ballistic transfer characteristics $I_d - V_{gs}$ at $V_{ds} = 0.7 \text{ V}$ for *p*-type BP FETs as in (a) at different misalignment angles δ . (d) Same as (c), but for *n*-type FETs.

III. RESULTS

As an example to illustrate the influence of orientation misalignments, we designed single-gate BP FETs loosely inspired by the specifications of the International Roadmap for Devices and Systems, as shown in Fig. 2(a). A gate length $L_g = 15 \text{ nm}$ was chosen to minimize source-to-drain leakages, which are not the subject of this study. All devices have a total length $L_{tot} \approx 40 \text{ nm}$. The top oxide has an equivalent oxide thickness $EOT = 0.6 \text{ nm}$ that ensures an excellent electrostatic control. Source and drain extensions are doped with a

donor/acceptor carrier concentration of $5 \times 10^{13} \text{ cm}^{-2}$. We found that such high values do not artificially boost the ON-current [12]. The OFF-state current is fixed to $0.1 \mu\text{A}/\mu\text{m}$.

All simulations were carried out at a supply voltage $V_{ds} = 0.7 \text{ V}$ and at room temperature. In Fig. 2(a) only the P atoms belonging to the 2-D channels enter the NEGF framework. The other layers are accounted for through Poisson's equations. The source and drain contact resistances are assumed to be negligibly small. Realistic top or side contacts might influence the dependence of the current on the transport direction, but adding them is not compatible with the chosen MLWF approach where the same unit cell is repeated to construct the device channel. Similarly, other potentially relevant effects such as the formation of direction-dependent crystal or edge defects are not considered here because their treatment significantly increases the computational burden.

Six different transport directions with a misalignment angle $\delta \in \{0^\circ, 20^\circ, 36^\circ, 55^\circ, 71^\circ, 90^\circ\}$ w.r.t. the optimal direction are considered. The ON-state currents of the different *n*- and *p*-type transistors are reported in Fig. 2(b) as a function of δ , with and without CIS and electron/hole-phonon scattering. For simplicity, the electrostatic potentials without scattering are used in both types of calculation. Finally, to enable rapid convergence of the NEGF calculations, small impurity concentrations of $N_{imp} = 2.5 \times 10^{11} \text{ cm}^{-2}$ are assumed in all cases.

The corresponding $I_d - V_{gs}$ ballistic transfer characteristics are given in Figs. 2(c) and (d). It can be observed that the ON-state currents do not vary much for $\delta \leq 20^\circ$, even in the presence of scattering. Moreover, the current reduction, as compared to the highest possible value is limited to 30% for misalignment $\delta < 50^\circ$. The current degradation then rapidly increases to reach 60% or more at $\delta = 90^\circ$. This finding demonstrates that the performance loss does not linearly depend on the misalignment angle, thus allowing for a certain tolerance during the fabrication process.

The non-linear dependence of the ON-state current on the transport direction does not appear to be a consequence of CIS or electron/hole-phonon scattering, as confirmed by the corresponding electron and hole low-field mobility in Fig. 3(a). This quantity, calculated with the “dR/dL” method [27], exhibits a similar behavior as the ON-state current. It stays almost constant up to 20° , slightly decreases between 20° and 36° , before experiencing a faster reduction at greater angles. The same happens if the impurity concentration is increased to $N_{imp} = 1 \times 10^{12} \text{ cm}^{-2}$. These results tend to indicate that the non-linearity of the current is an intrinsic property of BP directly coming from its bandstructure.

To reveal the role played by the BP bandstructure, we start by extracting relevant physical quantities at the top-of-the-barrier location (ToB) of the simulated FETs according to [12]. First, we observed that the charge at the ToB is about the same, regardless of the misalignment angle, because the DOS effective mass is orientation-independent. This will be demonstrated later. An approximation for the gate capacitance can be derived from the slope of the ToB charge density. A value $C_g \approx 5.6 \mu\text{F}/\text{cm}^2$ is found in all cases, close to the oxide capacitance $C_{ox} \approx 5.9 \mu\text{F}/\text{cm}^2$.

The ON-state current variations can be explained by ap-

proximating the $E(\vec{k})$ bandstructure dispersion of the lowest conduction band or the highest valence band as a parabola with a δ -dependent inverse effective mass tensor ($1/m_\delta$)

$$E(\vec{k}) = E_0 \pm \frac{\hbar^2}{2} \vec{k}^T \left(\frac{1}{m_\delta} \right) \vec{k}. \quad (1)$$

The $+/-$ sign refers to the electron/hole case, the energy E_0 either to the CB minimum or VB maximum, and \hbar to Plank's reduced constant. In Eq. 1 $1/m_\delta$ is defined as

$$\frac{1}{m_\delta} = R_\delta^T \left(\frac{1}{m_{\delta=0^\circ}} \right) R_\delta, \quad R_\delta = \begin{pmatrix} \cos \delta & \sin \delta \\ -\sin \delta & \cos \delta \end{pmatrix} \quad (2)$$

where R_δ is a rotation matrix and $m_{\delta=0^\circ}^{-1} = \text{diag}(m_{\Gamma-X}^{-1}, m_{\Gamma-Y}^{-1})$, the inverse effective mass tensor for transport along the $\Gamma - X$ direction with $m_{\Gamma-X} = 0.16m_0$ ($0.14m_0$), and $m_{\Gamma-Y} = 1.20m_0$ ($4.46m_0$) for electrons (holes). These effective masses were extracted as in [12] for an electron/hole population of $\sim 1.5e13 \text{ cm}^{-2}$. The transport effective mass $m_t(\delta)$ along any direction can be computed from Eq. 2 as [9]

$$\frac{1}{m_t(\delta)} = \frac{\sin^2 \delta}{m_{\Gamma-Y}} + \frac{\cos^2 \delta}{m_{\Gamma-X}} \quad (3)$$

By combining Eq. 1 and 2 the 2D DOS can be written as

$$DOS_{2D}(\epsilon) = \frac{\sqrt{m_{\Gamma-X} m_{\Gamma-Y}}}{\pi \hbar^2} H(\pm(\epsilon - E_0)) \quad (4)$$

Here, H is the Heavy-side function. It can be seen that the DOS only depends on the effective masses along the principle axes of the ellipses describing the bands, not on δ . This is why the gate capacitance, and the electrostatics too, are the same for all transport directions.

Next, an analytical expression is derived for the δ -dependent current

$$I(\delta) = \frac{e_0}{\pi \sqrt{m_t(\delta)}} \int d\epsilon DOS_{2D}(\epsilon) f(\epsilon, \epsilon_{F,S}) \times \sqrt{\pm 2(\epsilon - E_0 - \epsilon_{ToB})} \quad (5)$$

where e_0 is the elementary charge, ϵ_{ToB} the V_{gs} -dependent shift of the ToB energy, $f(\epsilon, \epsilon_{F,S})$ the Fermi distribution function, and $\epsilon_{F,S}$ the Fermi level in the source. From Eq. 5 it can be inferred that the current I_d should linearly depend on $1/\sqrt{m_t(\delta)}$ because the DOS is the same for all misalignment angles. This linear dependence can be observed in Fig. 3(b), where the ON-state currents from Fig. 2(b) are reported.

We then use Eq. 4 and 5 to extract m_{DOS} and $m_t(\delta)$, following the procedure outlined in [12]. The results are compared to $m_t(\delta)$, as calculated with Eq. 3, in Fig. 3(c). An excellent agreement is demonstrated. Key point is that $m_t(\delta)$ exhibits a plateau for $\delta \leq 20^\circ$, which reflect into an almost stable current in this range. Hence, Figs. 3(b) and (c) validate the form of Eq. 5.

The latter is finally recalled to compute the misalignment-induced current reductions w.r.t. to the maximum current value for any 2D material with an ellipsoidal bandstructure similar to BP. A map of the current reductions as a function of the $m_{\Gamma-X}/m_{\Gamma-Y}$ ratio and the misalignment angle δ is presented in Fig. 3(d) under the assumption of a fixed DOS. It can

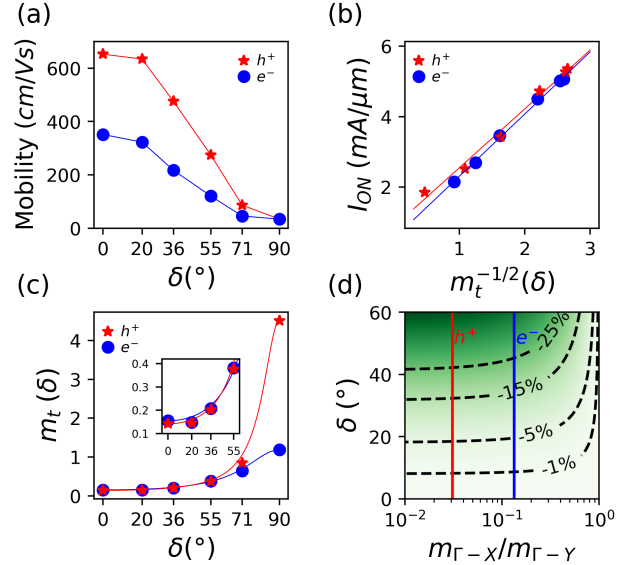


Fig. 3. (a) Charged impurity and electron/hole-phonon limited low-field mobility of electrons and holes in BP as a function of the transport direction. An impurity concentration $N_{imp}=2.5e11 \text{ cm}^{-2}$ is assumed. (b) ON-state current from Fig. 2(b) versus $1/\sqrt{m_t(\delta)}$. A linear dependence between them is clearly visible. (c) Transport effective mass $m_t(\delta)$ vs. δ as obtained from Eq. 4 and 5 (symbols) and as calculated with Eq. 3 (lines). (d) Current reduction w.r.t. $\delta = 0^\circ$ as a function of the $m_{\Gamma-X}/m_{\Gamma-Y}$ ratio and the alignment δ , as computed with Eq. 5. The dashed lines represent specific current reductions. The effective mass ratios of BP are indicated by the vertical solid lines.

be seen that for $m_{\Gamma-X}/m_{\Gamma-Y} < 0.1$ the ON-state current only marginally decreases up to $\delta \leq 20^\circ$, by 25% if the misalignment is pushed to 40° . It is clear that the magnitude of the ON-state current depends on the DOS of each 2D material. Nevertheless, a region where the current is almost insensitive to the misalignment angle can be expected in all cases.

IV. CONCLUSION

The effect of orientation misalignment caused by bandstructure anisotropies has been studied for n - and p -type black phosphorus FETs. A reduction of the ON-state current below 30% is found for misalignment angles $\delta \leq 50^\circ$, while the performance remains excellent for $\delta \leq 20^\circ$, with and without scattering. The effective mass along the transport direction explains this behavior, which does not display a strong dependence on electron/hole-phonon and charged impurity scattering. For materials with a similar ellipsoidal bandstructure as BP, regardless of the $m_{\Gamma-X}/m_{\Gamma-Y}$ ratio, minor current degradations are foreseen for misalignment angles δ up to 20° .

V. ACKNOWLEDGMENTS

This research was supported by the Swiss National Science Foundation (SNSF) under Grant No. 200021_175479 (ABIME) and under the NCCR MARVEL. We acknowledge CSCS for awarding us access to Piz Daint under project s876.

REFERENCES

- [1] K. S. Novoselov, A. K. Geim, S. V. Morozov, D. Jiang, Y. Zhang, S. V. Dubonos, I. V. Grigorieva, and A. A. Firsov, "Electric field effect in atomically thin carbon films," *Science*, vol. 306, no. 5696, pp. 666–669, 2004. [Online]. Available: <https://science.sciencemag.org/content/306/5696/666>
- [2] B. Radisavljevic, A. Radenovic, J. Brivio, V. Giacometti, and A. Kis, "Single-layer mos₂ transistors," *Nature Nanotechnology*, vol. 6, no. 3, pp. 147–150, Mar 2011. [Online]. Available: <https://doi.org/10.1038/nnano.2010.279>
- [3] L. Li, Y. Yu, G. J. Ye, Q. Ge, X. Ou, H. Wu, D. Feng, X. H. Chen, and Y. Zhang, "Black phosphorus field-effect transistors," *Nature Nanotechnology*, vol. 9, no. 5, pp. 372–377, May 2014. [Online]. Available: <https://doi.org/10.1038/nnano.2014.35>
- [4] H. Liu, A. T. Neal, Z. Zhu, Z. Luo, X. Xu, D. Tománek, and P. D. Ye, "Phosphorene: An unexplored 2d semiconductor with a high hole mobility," *ACS Nano*, vol. 8, no. 4, pp. 4033–4041, 2014, pMID: 24655084. [Online]. Available: <https://doi.org/10.1021/nn501226z>
- [5] F. Xia, H. Wang, and Y. Jia, "Rediscovering black phosphorus as an anisotropic layered material for optoelectronics and electronics," *Nature Communications*, vol. 5, no. 1, p. 4458, Jul 2014. [Online]. Available: <https://doi.org/10.1038/ncomms5458>
- [6] Y. Liu, T. Low, and P. P. Ruden, "Mobility anisotropy in monolayer black phosphorus due to scattering by charged impurities," *Phys. Rev. B*, vol. 93, p. 165402, Apr 2016. [Online]. Available: <https://link.aps.org/doi/10.1103/PhysRevB.93.165402>
- [7] N. Haratipour, Y. Liu, R. J. Wu, S. Namgung, P. P. Ruden, K. A. Mkhoyan, S. Oh, and S. J. Koester, "Mobility anisotropy in black phosphorus mosfets with hfo₂ gate dielectrics," *IEEE Transactions on Electron Devices*, vol. 65, no. 10, pp. 4093–4101, 2018.
- [8] J. Qiao, X. Kong, Z.-X. Hu, F. Yang, and W. Ji, "High-mobility transport anisotropy and linear dichroism in few-layer black phosphorus," *Nature Communications*, vol. 5, no. 1, p. 4475, Jul 2014. [Online]. Available: <https://doi.org/10.1038/ncomms5475>
- [9] P. Wu, T. Ameen, H. Zhang, L. A. Bendersky, H. Ilatikhameneh, G. Klimeck, R. Rahman, A. V. Davydov, and J. Appenzeller, "Complementary black phosphorus tunneling field-effect transistors," *ACS Nano*, vol. 13, no. 1, pp. 377–385, 2019. [Online]. Available: <https://doi.org/10.1021/acsnano.8b06441>
- [10] H. Ilatikhameneh, T. Ameen, B. Novakovic, Y. Tan, G. Klimeck, and R. Rahman, "Saving moore's law down to 1 nm channels with anisotropic effective mass," *Scientific Reports*, vol. 6, no. 1, p. 31501, Aug 2016. [Online]. Available: <https://doi.org/10.1038/srep31501>
- [11] N. Mounet, M. Gibertini, P. Schwaller, D. Campi, A. Merkys, A. Marrazzo, T. Sohier, I. E. Castelli, A. Cepellotti, G. Pizzi, and N. Marzari, "Two-dimensional materials from high-throughput computational exfoliation of experimentally known compounds," *Nature Nanotechnology*, vol. 13, no. 3, pp. 246–252, Mar 2018. [Online]. Available: <https://doi.org/10.1038/s41565-017-0035-5>
- [12] C. Klinkert, A. Szabo, C. Stieger, D. Campi, N. Marzari, and M. Luisier, "2-d materials for ultrascaled field-effect transistors: One hundred candidates under the ab initio microscope," *ACS Nano*, vol. 14, no. 7, pp. 8605–8615, 2020, pMID: 32530608. [Online]. Available: <https://doi.org/10.1021/acsnano.0c02983>
- [13] F. Liu, Y. Wang, X. Liu, J. Wang, and H. Guo, "Ballistic transport in monolayer black phosphorus transistors," *IEEE Transactions on Electron Devices*, vol. 61, no. 11, pp. 3871–3876, 2014.
- [14] K. Lam, Z. Dong, and J. Guo, "Performance limits projection of black phosphorous field-effect transistors," *IEEE Electron Device Letters*, vol. 35, no. 9, pp. 963–965, 2014.
- [15] R. Quhe, Q. Li, Q. Zhang, Y. Wang, H. Zhang, J. Li, X. Zhang, D. Chen, K. Liu, Y. Ye, L. Dai, F. Pan, M. Lei, and J. Lu, "Simulations of quantum transport in sub-5-nm monolayer phosphorene transistors," *Phys. Rev. Applied*, vol. 10, p. 024022, Aug 2018. [Online]. Available: <https://link.aps.org/doi/10.1103/PhysRevApplied.10.024022>
- [16] R. Wan, X. Cao, and J. Guo, "Simulation of phosphorene schottky-barrier transistors," *Applied Physics Letters*, vol. 105, no. 16, p. 163511, 2014. [Online]. Available: <https://doi.org/10.1063/1.4900410>
- [17] M. Luisier and G. Klimeck, "Atomistic full-band simulations of silicon nanowire transistors: Effects of electron-phonon scattering," *Phys. Rev. B*, vol. 80, p. 155430, Oct 2009. [Online]. Available: <https://link.aps.org/doi/10.1103/PhysRevB.80.155430>
- [18] G. Kresse and J. Furthmüller, "Efficient iterative schemes for ab initio total-energy calculations using a plane-wave basis set," *Phys. Rev. B*, vol. 54, pp. 11169–11186, Oct 1996. [Online]. Available: <https://link.aps.org/doi/10.1103/PhysRevB.54.11169>
- [19] A. A. Mostofi, J. R. Yates, Y.-S. Lee, I. Souza, D. Vanderbilt, and N. Marzari, "wannier90: A tool for obtaining maximally-localised wannier functions," *Computer Physics Communications*, vol. 178, no. 9, pp. 685 – 699, 2008. [Online]. Available: <http://www.sciencedirect.com/science/article/pii/S0010465507004936>
- [20] C. Stieger, "Ab-initio quantum transport simulations with tight-binding-like hamiltonians," Ph.D. dissertation, ETH Zurich, Zurich, 2019.
- [21] J. P. Perdew, K. Burke, and M. Ernzerhof, "Generalized gradient approximation made simple," *Phys. Rev. Lett.*, vol. 77, pp. 3865–3868, Oct 1996. [Online]. Available: <https://link.aps.org/doi/10.1103/PhysRevLett.77.3865>
- [22] M. Kuisma, J. Ojanen, J. Enkovaara, and T. T. Rantala, "Kohn-sham potential with discontinuity for band gap materials," *Phys. Rev. B*, vol. 82, p. 115106, Sep 2010. [Online]. Available: <https://link.aps.org/doi/10.1103/PhysRevB.82.115106>
- [23] G. Gaddemane, W. G. Vandenberghe, M. L. Van de Put, S. Chen, S. Tiwari, E. Chen, and M. V. Fischetti, "Theoretical studies of electronic transport in monolayer and bilayer phosphorene: A critical overview," *Phys. Rev. B*, vol. 98, p. 115416, Sep 2018. [Online]. Available: <https://link.aps.org/doi/10.1103/PhysRevB.98.115416>
- [24] Y. Lee, S. Fiore, and M. Luisier, "Ab initio mobility of single-layer mos₂ and ws₂: comparison to experiments and impact on the device characteristics," in *2019 IEEE International Electron Devices Meeting (IEDM)*, 2019, pp. 24.4.1–24.4.4.
- [25] Z.-Y. Ong and M. V. Fischetti, "Mobility enhancement and temperature dependence in top-gated single-layer mos₂," *Phys. Rev. B*, vol. 88, p. 165316, Oct 2013. [Online]. Available: <https://link.aps.org/doi/10.1103/PhysRevB.88.165316>
- [26] A. Szabó, R. Rhyner, and M. Luisier, "Ab initio simulation of single- and few-layer mos₂ transistors: Effect of electron-phonon scattering," *Phys. Rev. B*, vol. 92, p. 035435, Jul 2015. [Online]. Available: <https://link.aps.org/doi/10.1103/PhysRevB.92.035435>
- [27] K. Rim, S. Narasimha, M. Longstreet, A. Mocuta, and J. Cai, "Low field mobility characteristics of sub-100 nm unstrained and strained si mosfets," in *Digest. International Electron Devices Meeting.*, 2002, pp. 43–46.